Neuroscience 559 (2024) 263–271

Contents lists available at ScienceDirect

Neuroscience

journal homepage: www.elsevier.com/locate/nsc

Disturbances of thalamus and prefrontal cortex contribute to cognitive aging: A structure-function coupling analysis based on KL divergence

Weifang Cao [a,b,c,1], Jinpeng Niu [a,c,1], Yong Liang [b], Dong Cui [c], Qing Jiao [c], Zhen Ouyang [c], Guanghui Yu [c], Li Dong [a], Cheng Luo [a,*]

[a] School of Life Science and Technology, University of Electronic Science and Technology of China, Chengdu 611731, China
[b] Institute of Electronic and Information Engineering of Guangdong, University of Electronic Science and Technology of China, Dongguan 523000, China
[c] School of Radiology, Shandong First Medical University & Shandong Academy of Medical Sciences, Tai'an 271016, China

ARTICLE INFO

Keywords:
Aging
Distribution similarity
Cognition
Prefrontal cortex
Thalamus

ABSTRACT

Normal aging is accompanied by changes in brain structure and function associated with cognitive decline. Structural and functional abnormalities, particularly the prefrontal cortex (PFC) and subcortical regions, contributed to cognitive aging. However, it remains unclear how the synchronized changes in structure and function of individual brain regions affect the cognition in aging. Using 3D T1-weighted structural data and movie watching functional magnetic resonance imaging data in a sample of 422 healthy individuals (ages from 18 to 87 years), we constructed regional structure–function coupling (SFC) of cortical and subcortical regions by quantifying the distribution similarity of gray matter volume (GMV) and amplitude of low-frequency fluctuation (ALFF). Further, we investigated age-related changes in SFC and its relationship with cognition. With aging, increased SFC localized in PFC, thalamus and caudate nucleus, decreased SFC in temporal cortex, lateral occipital cortex and putamen. Moreover, the SFC in the PFC was associated with executive function and thalamus was associated with the fluid intelligence, and partially mediated age-related cognitive decline. Collectively, our results highlight that tighter structure–function synchron of the PFC and thalamus might contribute to age-related cognitive decline, and provide insight into the substrate of the thalamo-prefrontal pathway with cognitive aging.

Introduction

Alternations in brain structure and function across adult aging are associated with cognitive decline, such as executive function and cognitive flexibility (Blazer et al., 2015). The prefrontal cortex (PFC) is considered to be a key structure for the performance of executive function, conducting top-down signaling through neurons to control the activity of other cortical and subcortical structures (Funahashi and Andreau, 2013). By integrating information from the cerebral cortex, the thalamus is involved in multiple cognitive processes, such as decision making and cognitive flexibility (Antonucci et al., 2021). Normal aging is accompanied by abnormal changes in the morphology and excitability of neurons in the PFC and thalamus (Richardson et al., 2021; Uylings and de Brabander, 2002). The function of the neurons is determined by the structure and arrangement of neuronal populations, similarly, brain function is supported and constrained by anatomical structure (Suarez et al., 2020). Evidences from cognitive neuroscience in healthy and neurological disease populations showed that abnormal brain structure–function coupling (SFC) was associated with impaired cognitive function (Kulik et al., 2022; Sun et al., 2022). Therefore, elucidating the relationship between brain SFC and cognitive function has important implications for understanding the neural mechanisms of cognitive decline in aging and neurological diseases.

Magnetic resonance imaging (MRI) has been used to reveal brain structural and functional characteristics. The coupling of brain structure and function is considered to be a fundamental feature that reflects the integrity of neural signals (Liu et al., 2022). Gray matter, containing a large number of neuronal cell bodies, nerve fibers, glial cells and synapses, is a major component of the central nervous system, and the gray matter volume (GMV) reflects morphological characteristics of neurons, such as the number of nerve cells and dendrite density (Bota et al., 2005; Uylings HB and de Brabander, 2002). Recently, structural MRI (sMRI)

* Corresponding author at: University of Electronic Science and Technology of China, Chengdu, China.
E-mail address: chengluo@uestc.edu.cn (C. Luo).
[1] Weifang Cao and Jinpeng Niu contributed equally to this work.

https://doi.org/10.1016/j.neuroscience.2024.09.004
Received 12 January 2024; Accepted 1 September 2024
Available online 3 September 2024

studies have used GMV to reveal abnormal and pathology-specific changes in brain structure in healthy and neurological disease populations (Wan et al., 2020; Yu et al., 2021). An 8-year longitudinal MRI study showed that decreased GMV in the frontal and temporal lobes was associated with decreased processing speed in older adults (Leong et al., 2017). Hughes et al. showed that atrophy of the frontal thalamo-cortical circuit may explain age-related impairments in attention and executive function (Hughes et al., 2012). Meanwhile, functional magnetic resonance imaging (fMRI) studies have shown that age-related changes of brain function were associated with cognitive decline (Cohen et al., 2019; Fan et al., 2022). Amplitude of low-frequency fluctuation (ALFF) depicts amplitude or regional synchronization of automatic neural oscillations, revealing the level of spontaneous neuronal activity of brain regions in different states (Wang et al., 2021; Zang et al., 2007). Xing et al. has shown that increased ALFF in PFC in older adults was associated with worse immediate recall and recognition (Xing et al., 2022). Compared to younger adults, reduced ALFF in the superior parietal and middle frontal gyrus is associated with poorer executive function in older adults (Fan et al., 2022). Hence, the GMV and ALFF of local brain regions reflect the structural and functional activity characteristics of neurons, and quantifying synchronized changes of GMV and ALFF is helpful to understand the influence of brain SFC changes on cognitive function in aging and neurological diseases.

In the present study, we hypothesize that SFCs of the PFC and thalamus change across adults aging and are associated with cognitive decline. Recently, movie-watching state fMRI allows revealing the functional activity of the brain in close-to-daily-life conditions, and has advanced the understanding of human cognitive function in neuroimaging studies (Geerligs et al., 2018; Jaaskelainen et al., 2021). Therefore, using sMRI and movie-watching state fMRI data from a group of healthy participants (18–87 years old), we first constructed regional SFC by quantifying the distribution similarity of GMV and ALFF based on Kullback–Leibler (KL) divergence. Second, we performed general linear model (GLM) analysis to investigate age-related changes of regional SFC. Finally, we used partial correlation analysis and mediation analysis to detect the relationship between regional SFC and cognition. The schematic diagram of data processing and analysis is shown in Fig. 1.

Methods

Participants

Six hundred forty-seven healthy participants were recruited from the Cambridge Centre for Ageing and Neuroscience (Cam-CAN, https://www.cam-can.org/) project (Shafto et al., 2014). The exclusion criteria included the following: low performance (less than 25 score) in the Mini-Mental State Exam (MMSE), with severe memory defect, poor hearing (failing to hear 35 dB in either ear), non-native English-speakers or nonbilingual English-speakers from birth, consent difficulties for next stage, self-reported substance abuse, with serious head injury, with MRI contraindications and serious neurological and psychiatric disorders. In addition, eighty participants were excluded due to the missing fluid intelligence scores, and one hundred forty-five participants were excluded due to poor data quality and preprocessing (for details see MRI data preprocessing section). Finally, four hundred twenty-two participants were included in the present study (Table 1). Written informed consent was obtained from all participants, and ethical approval for the study was obtained from the local ethics committee, Cambridgeshire 2 Research Ethics Committee (reference: 10/H0308/50). And this study was conducted in compliance with the Helsinki Declaration.

Cognitive measures

Fluid intelligence reflects an individual's ability to respond to complex situations. In the present study, fluid intelligence was measured using the Cattell Culture Fair Test, a pen-and-paper test that contains four subtests with a series of nonverbal distractions, including series completion (3 min), classification (4 min), matrices (3 min) and conditions (2.5 min). In each trial, participants chose a response from multiple options and recorded it on an answer sheet. A correct response was given a score of 1 (46 scores in total) (Shafto et al., 2014).

Reaction time (RT) was measured with a speed choice RT task (Shafto et al., 2014). In the task, participants were required to response to 1 of 4 possible cued fingers as quickly as possible with a 4-button response box. A total of 67 trials were conducted, with maximum 3 s response time of each trial and mean 3.7 s inter-trial interval. RT was defined as the time from stimulus onset to button press. The intra-individual mean RT (mRT) was finally calculated for each participant from individual trials. Data were missing for 37 participants on the choice RT task (n = 385).

MRI data acquisition

All MRI scans were performed on a 3 T Siemens TIM Trio System with a 32-channel head coil. A high-resolution (1 mm × 1 mm × 1 mm) 3D T1-weighted image was acquired for each participant using a Magnetization Prepared Rapid Gradient Echo (MPRAGE) sequence with the following parameters: repetition time (TR) = 2250 ms, echo time (TE) = 2.99 ms, inversion time (TI) = 900 ms, field of view (FOV) = 256 mm × 240 mm × 192 mm, acceleration factor = 2, flip angle = 9 degrees, acquisition time = 4 min and 32 s. For the function scans, participants watched a black-and white television drama called "Bang! You're Dead". Functional images were acquired for each participant using a multi-echo, T2*-weighted EPI sequence (TR=2470 ms, 5 echoes [TE=9.4 ms, 21.2 ms, 33 ms, 45 ms, 57 ms], FOV=192 mm × 192 mm, voxel size = 3 mm × 3 mm × 4.44 mm, slice number = 32, slice thickness = 3.7 mm [20 % interslice gap], flip angle = 78 degrees) with an acquisition time of 8 min and 13 s.

MRI data preprocessing

For sMRI data, the preprocessing was carried out with the Computation Anatomy Toolbox (CAT12, Christian Gaser; Department of Psychiatry, University of Jena) based on Statistical Parametric Mapping 12 (SPM 12, https://www.fil.ion.ucl.ac.uk/spm/software/spm12). First, individual structural MRI images were segmented into GM, white matter (WM), and cerebrospinal fluid (CSF) using the unified segmentation model. Seventy-eight participants were excluded due to obvious artifacts and poor image segmentation. Total intracranial volume (TIV), calculated as the sum of GM, WM, and CSF volumes, was included as a covariate for further statistical analyses. Second, the GM images were normalized to the Montreal Neurological Institute (MNI) space with a high-dimensional "Diffeomorphic Anatomical Registration Through Exponential Lie Algebra (DARTEL)" approach and then nonlinearly modulated to compensate the effects of spatial normalization. Finally, the resulting GM images were resampled to 1.5 mm^3 voxels and spatially smoothed with a Gaussian kernel of 6 mm full width at half maximum (FWHM), resulting in a GMV map for each participant.

FMRI data were preprocessed using SPM12 and DPARSF software (Chao-Gan and Yu-Feng, 2010). Specifically, the first 5 time points were discarded to minimize the effect of magnetic field instability. The remaining images were slice-time corrected and then realigned for head motion correction. Sixty-seven participants were excluded due to excessive head motion, including translational movement > 2.5 mm or rotation > 2.5° or mean framewise displacement (mFD) > 0.5 mm. All realigned images were spatially normalized to the MNI space and resampled to the voxel size of 1.5 mm^3. The normalized images were then spatially smoothed with an isotropic 6 mm FWHM. At last, the linear trend was removed and the nuisance signals were regressed out, including WM signal, CSF signal, global signal and Friston-24 motion parameters.

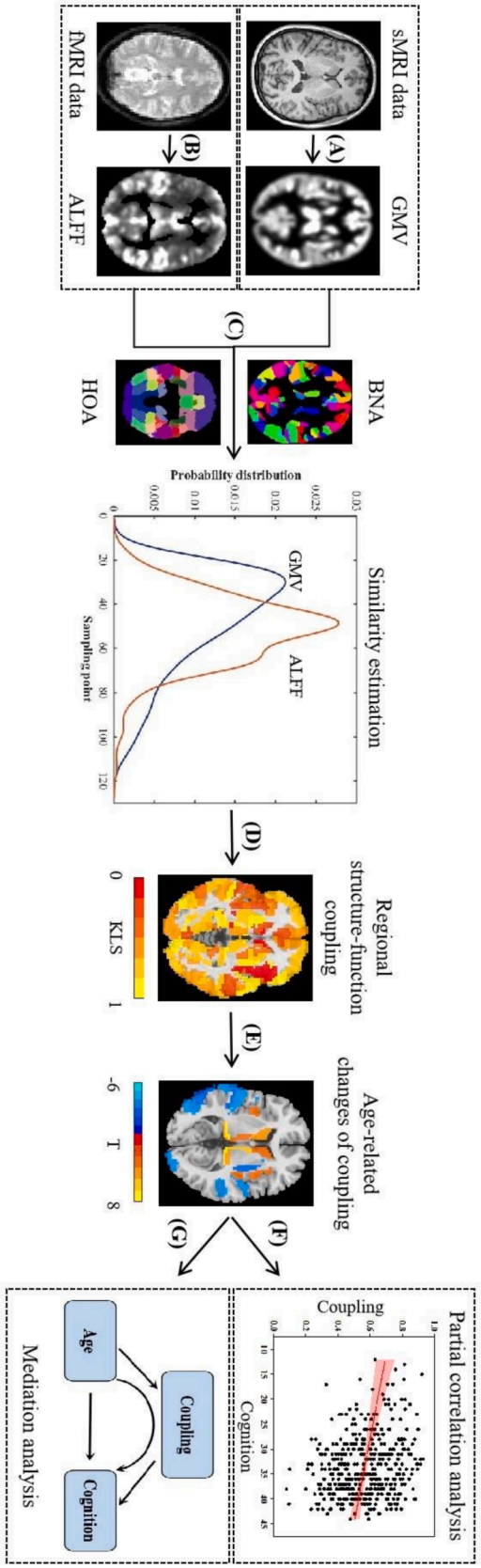

(caption on next column)

Fig. 1. The flowchart of the main analytic process. (A, B) Individual sMRI and fMRI data were preprocessed to obtain a GMV map and an ALFF map, respectively. (C) The GMV values and ALFF values of all voxels in each brain region (defined based on the BNA and HOA) were extracted to calculate the probability distribution function. (D) The similarity of GMV and ALFF probability distribution functions in each region was calculated based on Kullback–Leibler divergence, resulting in a regional SFC map. (E) A general linear model was used to investigate the relationship between SFC and age. (F, G) Partial correlation analysis and mediation analysis were performed to investigate the relationship between cognition and couplings of significant brain regions. sMRI, structural MRI; fMRI, functional MRI; GMV, gray matter volume; ALFF, amplitude of low frequency fluctuation; BNA, brainnectome atlas; HOA, Harvard-Oxford atlas; KLS, Kullback–Leibler divergence-based similarity; SFC, structure–function coupling.

Calculation of ALFF

An ALFF map was calculated for each participant using preprocessed fMRI data. Briefly, the time course of each voxel was converted to the frequency domain with fast Fourier transform to obtain the power spectrum. The square root of the power was calculated and averaged across 0.01–0.08 Hz. This averaged square root was regarded as the ALFF value for each voxel (Zang et al., 2007).

Calculation of regional SFC

A regional SFC map was constructed for each participant with a human Brainnetome atlas (BNA) and a structural brain atlas (Harvard-Oxford atlas, HOA), respectively (DN. K et al., 1998; Fan et al., 2016). BNA divided the brain into 210 cortical and 36 subcortical regions, and HOA included 96 cortical and 14 subcortical regions. For each participant, the GMV and ALFF values were first extracted for all voxels in each brain region. Then, the probability density functions of GMV and ALFF within each region were calculated separately based on a normal kernel function (*ksdensity* in MATLAB). The probability distribution functions (PDFs) were further calculated from the probability density functions. Finally, Kullback–Leibler (KL) divergence of the PDFs of GMV and ALFF within each region was calculated. KL divergence is a measure of the difference between two probability distributions in probability theory (Kong et al., 2014). Theoretically, the KL divergence of the distribution Q to P is defined as follows:

$$D_{KL}(P||Q) = \sum_{i=1}^{n} P(i) log \frac{P(i)}{Q(i)},$$

with P and Q are two PDFs and n is the number of sample points. In the present study, 2^7 sampling points was chosen conservatively as in previous studies (Wang et al., 2016). Since $D_{KL}\ (P||Q)$ is not equal to $D_{KL}\ (Q||P)$, a symmetric measure was derived as follows:

$$D_{KL}(P,Q) = \sum_{i=1}^{n} \left(P(i) log \frac{P(i)}{Q(i)} + Q(i) log \frac{Q(i)}{P(i)} \right).$$

Finally, the KL divergence was transformed into a similarity measure as follows:

$$KLS(P,Q) = e^{-D_{KL}(P,Q)},$$

with e is natural exponential. KL divergence-based similarity (KLS) ranges from 0 to 1, with higher values representing more similar distributions of GMV and ALFF. Moreover, the similarity of GMV and ALFF distributions in the whole brain was calculated for each participant and included as a covariate for further statistical analyses.

Statistical analysis

General linear model analysis

To investigate the relationship between regional SFC and age, a GLM

Table 1
Demographic data and cognitive measures of participants.

	Participant (n = 422)
Age range (year)	18–87
Male/Female	199/223
Education	
University	299
A' Levels	61
GCSE grade	57
None over 16	5
mFD	0.17 (0.08)
MMSE	29.11 (1.17)
Fluid intelligence	33.57 (6.16)
mRT (n = 385)	0.56 (0.13)

Values in parentheses are standard deviations. mFD, mean framewise displacement; MMSE, mini mental status examination; mRT, mean reaction time. According to the British education system: University—undergraduate or graduate degree; A' Levels—General Certificate of Education Advanced Level; GCSE grade—General Certificate of Secondary Education.

was used to fit the KLS value of each brain region over age/age^2. Meanwhile, gender, education level, mFD, TIV and brain-wide coupling were added as covariates in the model (Equation (1). T values were calculated for each regression coefficient to measure the impact of age (linear and quadratic) on regional SFC. FDR correction was performed for multiple comparisons with $p < 0.05$.

$$Y_{KLS} = \beta_1 \cdot X_{age} + \beta_2 \cdot X_{age^2} + \beta_3 \cdot X_{sex} + \beta_4 \cdot X_{edu} + \beta_5 \cdot X_{mFD} + \beta_6 \cdot X_{TIV} + \beta_7 \cdot X_{coup} + c \quad (1)$$

Partial correlation analysis

To further investigate the relationship between the regional SFC and cognitive function. Partial correlation analyses were performed separately for fluid intelligence, mRT and regional SFC showed age-related alternations. Similarly, gender, education level, mFD, TIV and brain-wide coupling were added as covariates. FDR correction was performed for multiple comparisons with $p < 0.05$.

Mediation analysis

To further verify the assumption that the age-related alternations of regional SFC are associated with cognitive decline. Bootstrapped mediation analyses were performed to investigate whether age-related changes in fluid intelligence, mRT were mediated by alternations of regional SFC. First, the effects of covariates (same as used in GLM analysis) on the independent (X, age), dependent (Y, cognition) and mediating (M, regional SFC) variables were regressed out. The residuals were then normalized and used in mediation analysis. Finally, the total effect of age on cognition (path c), the relationship between regional SFC and age (path a), the relationship between regional SFC and cognition (path b), and the direct effect of age on cognition while including regional SFC as a mediator (path c') were examined. The significance of the indirect effect (path a*b) of age on cognition through the regional SFC was tested with a bootstrapping analysis (resampled 10,000 times). Mediation analysis was performed using the *Mediation ToolBox* (https://github.com/canlab/MediationToolbox).

Split-half validation analysis

To investigate the reproducibility and repeatability of the relationship between regional SFC and age, cognitive function, half the participants were randomly selected (Table S3). The individual regional SFC map was constructed for each participant based on BNA. GLM analysis was conducted to explore age-related changes of regional SFC. The degree of overlapping regions with discovery analysis was measured by the odds ratio. Partial correlation analysis and mediation analysis were also conducted to explore the relationship between regional SFC and fluid intelligence, mRT. The codes for statistical analyses in this study have been shared on github (https://github.com/Niu619/Structure-function-coupling).

Results

Age-related changes of regional SFC

We used a GLM to quantify the relationship between regional SFC and age. In both atlases, significant positive correlations were found in PFC, insular cortex and subcortical regions, including superior frontal gyrus (SFG), thalamus and caudate nucleus; significant negative correlations were found in lateral occipital cortex (LOC), putamen, nucleus accumbens (NAC) and temporal cortex, which mainly included superior temporal gyrus (STG), middle temporal gyrus (MTG), and inferior temporal gyrus (ITG) (Fig. 2 and Table S1, S2). In BNA, significant positive correlation was also found in insula, and negative correlation was found in paracentral lobule (Fig. 2A and Table S1). In validation analysis, the brain regions whose coupling showed significant correlation with age were highly overlapped with that in discovery analysis: odds ratio = 39, $p < 0.0001$ (Fig. S1 B, C). Specifically, positive correlations were found in part of SFG, thalamus, insula and caudate nucleus; negative correlations were found in part of STG, ITG, LOC and putamen (Fig. S1 A).

Meanwhile, we examined the quadratic relationship between regional SFC and age. In BNA, the coupling in left dorsal insula was positively correlated with age, while the couplings in right STG and bilateral caudal temporal thalamus were negatively correlated with age (Fig. S2 A). In HOA, positive correlations with age were found in right superior LOC, while negative correlations were found in right temporal pole, right posterior STG, right inferior LOC and right putamen (Fig. S2 B). Similar to discovery analysis, the coupling in left dorsal insula was also positively correlated with age in validation analysis, and the couplings in right STG and right caudal temporal thalamus showed negative correlation with age (Fig. S3).

Relationship between regional SFC and fluid intelligence

We used partial correlation analysis and mediation analysis to quantify the relationship between regional SFC and fluid intelligence. In both atlases, the coupling in STG, ITG and left LOC showed positive correlation with fluid intelligence, while negative correlations were found in thalamus and caudate nucleus (FDR correction with $p < 0.05$, Table S4). In BNA, positive correlation was also found in left NAC, and negative correlations were found in right SFG and part of insular. Mediation analysis showed that age-related decline in fluid intelligence was partially mediated by higher SFC in left occipital thalamus and right medial prefrontal thalamus (Fig. 3). In HOA, higher SFC in thalamus also partially mediated age-related decline in fluid intelligence (Fig. S3). In validation analysis, the couplings of left occipital thalamus and right medial prefrontal thalamus exhibited significant negative correlation with fluid intelligence, r_{209} = -0.31, $p < 0.0001$, and r_{209} = -0.21, p = 0.0025, respectively. Meanwhile, higher SFCs partially mediate age-related decline in fluid intelligence (Fig. S4).

Relationship between regional SFC and RT

Similarly, we used partial correlation analysis and mediation analysis to quantify the relationship between regional SFC and RT. In both atlases, the SFC in part of left SFG, thalamus and right precentral gyrus (PrG) showed positive correlation with RT, while negative correlations were found in left ITG and left LOC (FDR correction with $p < 0.05$, Table S5). In BNA, positive correlation was also found in insula, and negative correlation was found in left fusiform gyrus. Mediation analysis showed that age-related increase in RT was partially mediated by higher SFC in left SFG (Fig. 4). In HOA, negative correlations were also found in

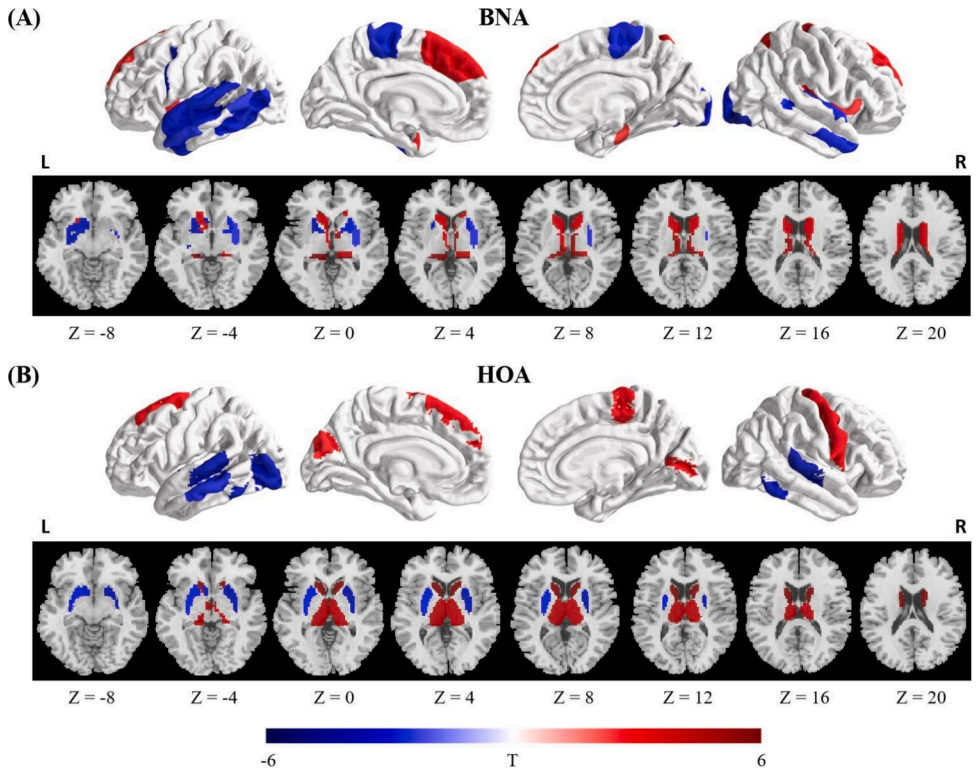

Fig. 2. Linear relationship between regional SFC and age. (A) and (B) display brain regions that exhibit significant changes in SFC with age in BNA and HOA, respectively. The warm (cool) color represents a positive (negative) correlation between regional SFC and age (FDR correction with $p < 0.05$). BNA, brainnectome atlas; HOA, Harvard-Oxford atlas; SFC, structure–function coupling; L, left; R, right.

part of right STG, left NAC and right putamen (FDR correction with $p < 0.05$, Table S5). Mediation analysis showed that higher SFCs in left SFG and right PrG partially mediated age-related increase in RT (Fig. 4). In validation analysis, the couplings of left SFG and left occipital thalamus exhibited significant positive correlation with RT, $r_{194} = 0.21$, $p = 0.0042$, and $r_{194} = 0.22$, $p = 0.0020$, respectively. Meanwhile, higher SFCs partially mediate age-related increase in RT (Fig. S5).

Discussion

In the current study, we investigated the effect of age-related SFC alternations on cognitive decline. With aging, we observed increased SFC in the PFC, thalamus and caudate nucleus, and decreased SFC in the temporal cortex, LOC and putamen. Furthermore, the SFCs of PFG, thalamus and caudate nucleus were negatively correlated with fluid intelligence, and positively correlated with RT, while the SFCs of STG, ITG and LOC were positively correlated with fluid intelligence, and negatively correlated with RT. Importantly, the SFCs of PFC and thalamus partially mediated age-related decline of executive function and fluid intelligence. Our results suggest that synchronized changes in structure and function of PFC and thalamus might contribute to age-related cognitive decline.

We constructed regional SFC and explored the age-related change pattern of coupling and its effect on cognitive decline. The coupling in several regions increased with age, including PFC, thalamus and caudate nucleus, and increased couplings were associated with the decline in cognition function. Evidence from rats and human have showed that the dendritic branches of PFC decrease with age, suggesting that the morphology of PFC is susceptible to aging (Grill and Riddle, 2002; Uylings and de Brabander, 2002). Meanwhile, Ca^{2+} homeostasis may be disrupted in aging PFC neurons and the amplitude of the action potential may decrease (Chang et al., 2005). Using functional-structural covariance network analysis, Marstaller et al. found that age-related decline in GMV was associated with reduced activity of prefrontal nodes in salience network and frontoparietal network (Marstaller et al., 2015). Therefore, the age-related increase of SFC in PFC suggests abnormal morphology and function of neurons in PFC. As a relay station, the macrostructure, microstructure and neural activity of the thalamus changes across the lifespan (Fama and Sullivan, 2015). Thalamus has extensive structural and functional connections to the cortical and subcortical regions, and the integrity of fibrous projections and functional connections decrease synchronously during aging (Menegaux et al., 2019; Niu et al., 2022). A longitudinal MRI study has shown that the volume of caudate nucleus decreases across the lifespan (Narvacan et al., 2017). Meanwhile, older adults with lower caudate nucleus activation performed worse on working memory tasks (Ducharme-Laliberte et al., 2022). Notably, Gu et al. found age-related decrease of structural and functional connectivity coupling (SC-FC coupling) in thalamus and caudate nucleus, which suggests reduced structural projection and compensatory functional links between the thalamus and caudate nucleus and other brain regions (Gu et al., 2021). However, increased SFC in thalamus and caudate nucleus suggests age-related regional atrophy and functional abnormalities. Taken together, increased couplings of PFC, thalamus and caudate nucleus during aging suggest synchronous changes in neuronal morphology and function, and SFC may provide additional insights into the age-related change patterns of brain coupling.

We also found that the SFCs of temporal cortex, LOC and putamen decrease with age, and decreased couplings were associated with the decline in cognition function. Evidence from sMRI study showed that gray matter atrophy occurs first in the temporal cortex during aging (Wan et al., 2020). Using pulsed arterial spin labeling MRI, Preibisch et al. found that cerebral blood flow in the temporal cortex was higher in healthy adults and increased with age (Preibisch et al., 2011). Increased regional neurophysiological activity requires higher metabolic demands, which are met through increased regional blood flow (Tak et al.,

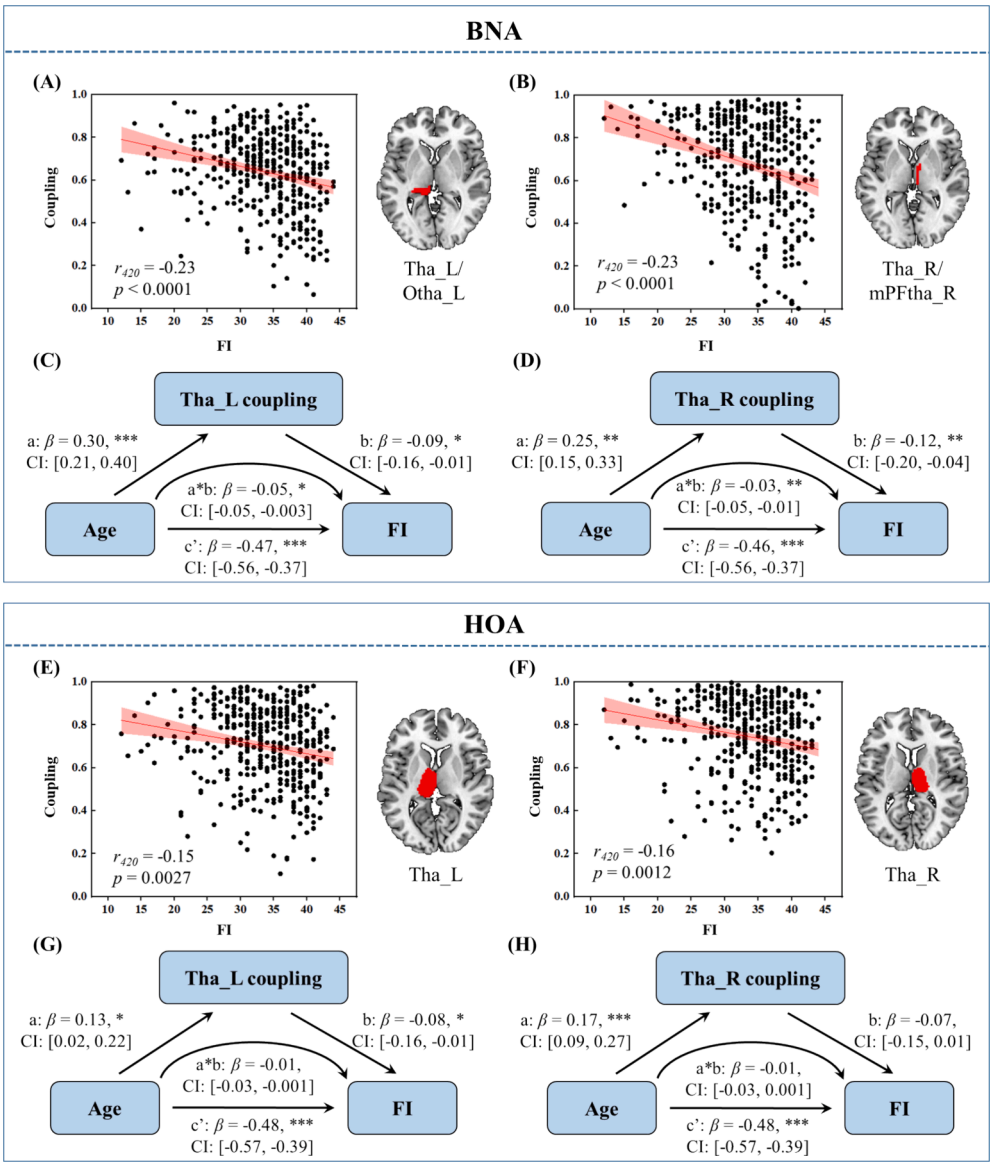

Fig. 3. Regional SFCs are associated with fluid intelligence. The SFCs of the thalamus, defined by BNA (A, B) and HOA (E, F) respectively, were significantly negatively correlated with fluid intelligence (FDR correction with $p < 0.05$). Age-related decline in fluid intelligence is partially mediated by higher SFC in thalamus, defined by BNA (C, D) and HOA (G, H), respectively. Mediation effects are reported as standardized regression coefficients, and the significance is identified with 95 % bootstrapped confidence intervals. * $p < 0.05$, ** $p < 0.01$, *** $p < 0.001$. Tha, thalamus; FI, fluid intelligence; BNA, brainnectome atlas; HOA, Harvard-Oxford atlas; SFC, structure–function coupling; L, left; R, right.

2015). Thus, the temporal cortex showed a coupling decrease with atrophy and increased neural activity during aging. Similarly, the putamen also showed age-related atrophy and increased local cerebral perfusion (Wang et al., 2019; Zhang et al., 2018). Using diffusion-weighted imaging (DTI) and fMRI, Baum et al. found that higher similarity in structural and functional connections in the occipital cortex was associated with better executive ability in adolescents (Baum et al., 2020). The process of myelination of synapses and fibers during brain development may affect the coupling of structural and functional connections, and fibers that complete myelination later are more susceptible to age-related changes or pathology (Baum et al., 2020; Gu et al., 2021).

The link between brain structure and function is a subject of great concern in cognitive neuroscience. Previous studies have quantified the link between structural and functional connectivity patterns of individual brain region, and found that the SC-FC coupling of brain regions is significantly correlated with cognitive function and behavioral performance (Suarez et al., 2020; Uddin, 2013). Gu et al. showcased that the SC-FC couplings of the bilateral medial cingulate cortex and supplementary motor area were negatively correlated with the composite cognitive scores (Gu et al., 2021). Medaglia et al. found that the consistency between functional signals and underlying network architecture of the anterior cingulate cortex and subcortical regions was associated with cognitive flexibility (Medaglia et al., 2018). Instead of measuring the consistency between the structural connectome and functional connectome, we constructed regional SFC by quantifying the distribution similarity between GMV and ALFF. We found that the SFC of PFC and thalamus was negatively correlated with cognitive function, while the SFC of temporal cortex was positively correlated with cognitive function. Overall, the anatomical structures of the brain are the basis for the completion of relevant neural activities and cognitive processes, and the SFC provides a new perspective to reveal cognitively related brain organization traits.

Using mediation analysis, we found that higher SFCs in the PFC and

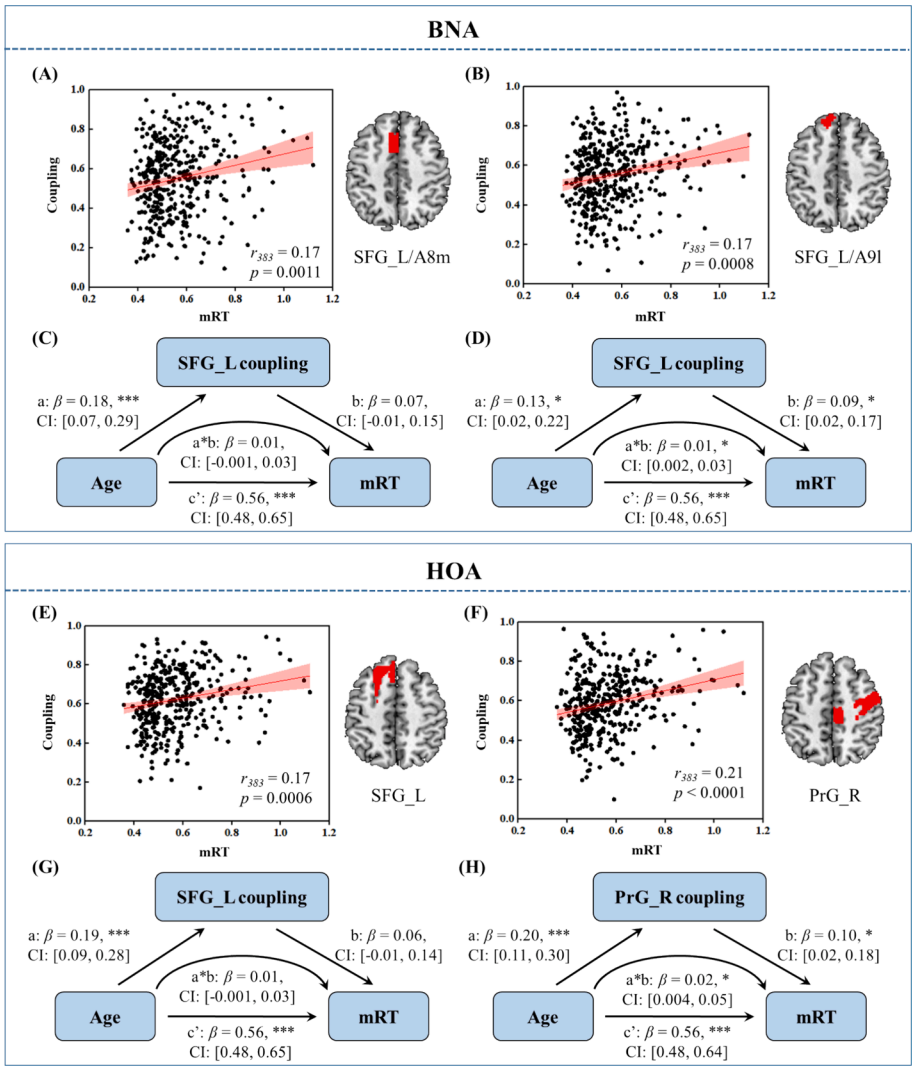

Fig. 4. Regional SFCs are associated with reaction time. The SFCs of the superior frontal gyrus and precentral gyrus, defined by BNA (A, B) and HOA (E, F) respectively, were significantly positively correlated with reaction time (FDR correction with $p < 0.05$). Age-related increase in reaction time is partially mediated by higher SFC in superior frontal gyrus and precentral gyrus, defined by BNA (C, D) and HOA (G, H), respectively. Mediation effects are reported as standardized regression coefficients, and the significance is identified with 95 % bootstrapped confidence intervals. * $p < 0.05$, ** $p < 0.01$, *** $p < 0.001$. SFG, superior frontal gyrus; PrG, precentral gyrus; mRT, mean reaction time; BNA, brainnectome atlas; HOA, Harvard-Oxford atlas; SFC, structure–function coupling; L, left; R, right.

thalamus partially mediated age-related cognitive decline. Functional abnormalities in the PFC have been shown to be associated with age-related decline of executive function and cognitive control (Li et al., 2022). The thalamus is a key node that supports a variety of cognitive functions and behaviors, such as executive function and processing speed (Antonucci, et al., 2021). Normal aging is accompanied by the shrinkage of regional thalamic volume, degeneration of microstructure and decrease of neural activity, which is related to the decline of information processing speed and memory (Fama and Sullivan, 2015). Moreover, the reciprocal connectivity between the thalamus and PFC plays an important role in the maintenance of sensory perception and cognitive function. Mediodorsal thalamus sustains the activity of the PFC, enhancing its excitability improves the performance in working memory tasks (Bolkan et al., 2017). Using DTI, Guberman et al. found that structural abnormalities in the thalamo-prefrontal pathway predicted working memory scores (Guberman et al., 2020). The integrity of the thalamo-prefrontal fiber connection predicted improvements in cognitive function after exercise training in middle-aged and older adults, which suggests that exercise training may primarily utilize fibers in the thalamo-prefrontal pathway to perform repetitive tasks (Wu et al., 2020). In summary, the integrity of the thalamo-prefrontal pathway is critical for the maintenance of cognitive function. Physical intervention and neural regulation of thalamo-prefrontal pathway may delay and improve cognitive decline in older adults.

The current study has certain limitations. First, GMV and ALFF were used to construct regional SFC in this study, age-related changes in similarity of more structural and functional features could be explored in the future, which might provide new insights into the underlying mechanisms of aging and neurological diseases. Second, according to Wang et al., 2^7 sampling points were conservatively chosen, and the KLS measure was used to estimate the similarity of the regional PDF (Wang et al., 2016). Future research is required to select different factors to examine unique insights into the brain's SFC. Finally, longitudinal studies are necessary to reveal the trajectory of brain development during aging and to elucidate the underlying mechanisms behind cognitive decline. We hope to replicate our findings using longitudinal data set in the future.

This study revealed increased SFCs of the PFC and thalamus across adults aging, and their synchronized changes in structure and function were significantly associated with age-related cognitive decline. Our findings suggest that abnormalities in the structure and function of neurons in the PFC and thalamus might indicate the underlying

pathophysiology of cognitive decline during aging, which provide important neuroimaging biomarkers for delaying and intervening cognitive aging.

Funding

This work was supported by the Funds for the China Postdoctoral Science Foundation (2022 M710625). Natural Science Foundation of Shandong Province (ZR2023MH294; ZR2023MH319). National Natural Science Foundation of China (81901730).

CRediT authorship contribution statement

Weifang Cao: Investigation, Writing – original draft. **Jinpeng Niu:** Data curation, Methodology. **Yong Liang:** Software. **Dong Cui:** Investigation. **Qing Jiao:** Funding acquisition, Methodology. **Zhen Ouyang:** Formal analysis. **Guanghui Yu:** Visualization. **Li Dong:** Conceptualization, Writing – review & editing. **Cheng Luo:** Funding acquisition, Project administration, Writing – review & editing.

Declaration of Competing Interest

The authors declare that they have no known competing financial interests or personal relationships that could have appeared to influence the work reported in this paper.

Acknowledgements

The authors are grateful to the Cam-CAN respondents and their primary care teams at Cambridge for their participation in this study.

Appendix A. Supplementary data

Supplementary data to this article can be found online at https://doi.org/10.1016/j.neuroscience.2024.09.004.

References

Antonucci, L.A., Penzel, N., Pigoni, A., Dominke, C., Kambeitz, J., Pergola, G., 2021. Flexible and specific contributions of thalamic subdivisions to human cognition. Neurosci. Biobehav. Rev. 124, 35–53.
Baum, G.L., Cui, Z., Roalf, D.R., Ciric, R., Betzel, R.F., Larsen, B., Cieslak, M., Cook, P.A., et al., 2020. Development of structure-function coupling in human brain networks during youth. PNAS 117, 771–778.
Blazer, D.G., Yaffe, K., Karlawish, J., 2015. Cognitive Aging. J. Am. Med. Assoc. 313.
Bolkan, S.S., Stujenske, J.M., Parnaudeau, S., Spellman, T.J., Rauffenbart, C., Abbas, A.I., Harris, A.Z., Gordon, J.A., et al., 2017. Thalamic projections sustain prefrontal activity during working memory maintenance. Nat. Neurosci. 20, 987–996.
Bota, M., Dong, H.W., Lw. s,, 2005. Brain architecture management system. Neuroinformatics 3, 15–48.
Chang, Y.M., Rosene, D.L., Killiany, R.J., Mangiamele, L.A., Luebke, J.I., 2005. Increased action potential firing rates of layer 2/3 pyramidal cells in the prefrontal cortex are significantly related to cognitive performance in aged monkeys. Cereb. Cortex 15, 409–418.
Chao-Gan, Y., Yu-Feng, Z., 2010. DPARSF: A MATLAB Toolbox for "Pipeline" Data Analysis of Resting-State fMRI. Front. Syst. Neurosci. 4, 13.
Cohen, R.A., Marsiske, M.M., Smith, G.E., 2019. Neuropsychology of aging. Handb. Clin. Neurol. 167, 149–180.
DN. K, N. L, N. M, J. B, J. M, Jr. CV (1998), Gyri of the human neocortex: an MRI-based analysis of volume and variance. Cereb Cortex 8:372–384.
Ducharme-Laliberte, G., Mellah, S., Boller, B., Belleville, S., 2022. More flexible brain activation underlies cognitive reserve in older adults. Neurobiol. Aging 113, 63–72.
Fama, R., Sullivan, E.V., 2015. Thalamic structures and associated cognitive functions: Relations with age and aging. Neurosci. Biobehav. Rev. 54, 29–37.
Fan, L., Li, H., Zhuo, J., Zhang, Y., Wang, J., Chen, L., Yang, Z., Chu, C., et al., 2016. The Human Brainnetome Atlas: A New Brain Atlas Based on Connectional Architecture. Cereb. Cortex 26, 3508–3526.
Fan, D., Liu, T., Jiang, J., Kochan, N.A., Wang, Y., Brodaty, H., Sachdev, P.S., Wen, W., 2022. Cognitive decline is associated with frequency-specific resting state functional changes in normal aging. Brain Imaging Behav. 16, 2120–2132.
Funahashi, S., Andreau, J.M., 2013. Prefrontal cortex and neural mechanisms of executive function. J. Physiol. Paris 107, 471–482.
Geerligs, L., Cam, C.A.N., Campbell, K.L., 2018. Age-related differences in information processing during movie watching. Neurobiol. Aging 72, 106–120.
Grill, J.D., Riddle, D.R., 2002. Age-related and laminar-specific dendritic changes in the medial frontal cortex of the rat. Brain Res. 937 (1–2), 8–21.
Gu, Z., Jamison, K.W., Sabuncu, M.R., Kuceyeski, A. (2021), Regional structural-functional connectome coupling is heritable and associated with age, sex and cognition in adults.
Gu, Z., Jamison, K.W., Sabuncu, M.R., Kuceyeski, A., 2021a. Heritability and interindividual variability of regional structure-function coupling. Nat. Commun. 12, 4894.
Guberman, G.I., Houde, J.C., Ptito, A., Gagnon, I., Descoteaux, M., 2020. Structural abnormalities in thalamo-prefrontal tracks revealed by high angular resolution diffusion imaging predict working memory scores in concussed children. Brain Struct. Funct. 225, 441–459.
Hughes, E.J., Bond, J., Svrckova, P., Makropoulos, A., Ball, G., Sharp, D.J., Edwards, A. D., Hajnal, J.V., et al., 2012. Regional changes in thalamic shape and volume with increasing age. Neuroimage 63, 1134–1142.
Jaaskelainen, I.P., Sams, M., Glerean, E., Ahveninen, J., 2021. Movies and narratives as naturalistic stimuli in neuroimaging. Neuroimage 224, 117445.
Kong, X.Z., Wang, X., Huang, L., Pu, Y., Yang, Z., Dang, X., Zhen, Z., Liu, J., 2014. Measuring individual morphological relationship of cortical regions. J. Neurosci. Methods 237, 103–107.
Kulik, S.D., Nauta, I.M., Tewarie, P., Koubiyr, I., van Dellen, E., Ruet, A., Meijer, K.A., de Jong, B.A., et al., 2022. Structure-function coupling as a correlate and potential biomarker of cognitive impairment in multiple sclerosis. Netw Neurosci 6, 339–356.
Leong, R.L.F., Lo, J.C., Sim, S.K.Y., Zheng, H., Tandi, J., Zhou, J., Chee, M.W.L., 2017. Longitudinal brain structure and cognitive changes over 8 years in an East Asian cohort. Neuroimage 147, 852–860.
Li, L., Huang, X., Xiao, J., Zheng, Q., Shan, X., He, C., Liao, W., Chen, H., et al., 2022. Neural synchronization predicts marital satisfaction. PNAS 119 e2202515119.
Liu, Z.-Q., Vázquez-Rodríguez, B., Spreng, R.N., Bernhardt, B.C., Betzel, R.F., Misic, B., 2022. Time-resolved structure-function coupling in brain networks. Communications Biology 5.
Marstaller, L., Williams, M., Rich, A., Savage, G., Burianova, H., 2015. Aging and large-scale functional networks: white matter integrity, gray matter volume, and functional connectivity in the resting state. Neuroscience 290, 369–378.
Medaglia, J.D., Huang, W., Karuza, E.A., Kelkar, A., Thompson-Schill, S.L., Ribeiro, A., Bassett, D.S., 2018. Functional alignment with anatomical networks is associated with cognitive flexibility. Nat. Hum. Behav. 2, 156–164.
Menegaux, A., Napiorkowski, N., Neitzel, J., Ruiz-Rizzo, A.L., Petersen, A., Muller, H.J., Sorg, C., Finke, K., 2019. Theory of visual attention thalamic model for visual short-term memory capacity and top-down control: Evidence from a thalamo-cortical structural connectivity analysis. Neuroimage 195, 67–77.
Narvacan, K., Treit, S., Camicioli, R., Martin, W., Beaulieu, C., 2017. Evolution of deep gray matter volume across the human lifespan. Hum. Brain Mapp. 38, 3771–3790.
Niu, J., Zheng, Z., Wang, Z., Xu, L., Meng, Q., Zhang, X., Kuang, L., Wang, S., et al., 2022. Thalamo-cortical inter-subject functional correlation during movie watching across the adult lifespan. Front. Neurosci. 16, 984571.
Preibisch, C., Sorg, C., Forschler, A., Grimmer, T., Sax, I., Wohlschlager, A.M., Perneczky, R., Forstl, H., et al., 2011. Age-related cerebral perfusion changes in the parietal and temporal lobes measured by pulsed arterial spin labeling. J. Magn. Reson. Imaging 34, 1295–1302.
Richardson, B.D., Sottile, S.Y., Caspary, D.M., 2021. Mechanisms of GABAergic and cholinergic neurotransmission in auditory thalamus: Impact of aging. Hear. Res. 402, 108003.
Shafto, M.A., Tyler, L.K., Dixon, M., Taylor, J.R., Rowe, J.B., Cusack, R., Calder, A.J., Marslen-Wilson, W.D., et al., 2014. The Cambridge Centre for Ageing and Neuroscience (Cam-CAN) study protocol: a cross-sectional, lifespan, multidisciplinary examination of healthy cognitive ageing. BMC Neurol. 14.
Suarez, L.E., Markello, R.D., Betzel, R.F., Misic, B., 2020. Linking structure and function in macroscale brain networks. Trends Cogn. Sci. 24, 302–315.
Sun, L., Liang, X., Duan, D., Liu, J., Chen, Y., Wang, X., Liao, X., Xia, M., et al., 2022. Structural insight into the individual variability architecture of the functional brain connectome. Neuroimage 259, 119387.
Tak, S., Polimeni, J.R., Wang, D.J., Yan, L., Chen, J.J., 2015. Associations of resting-state fMRI functional connectivity with flow-BOLD coupling and regional vasculature. Brain Connect. 5, 137–146.
Uddin, L.Q., 2013. Complex relationships between structural and functional brain connectivity. Trends Cogn. Sci. 17, 600–602.
Uylings, H.B., de Brabander, J.M., 2002. Neuronal changes in normal human aging and Alzheimer's disease. Brain Cogn. 49, 268–276.
Wan, M., Xia, R., Lin, H., Qiu, P., He, J., Ye, Y., Tao, J., Chen, L., et al., 2020. Volumetric and diffusion abnormalities in subcortical nuclei of older adults with cognitive frailty. Front. Aging Neurosci. 12, 202.
Wang, L., Feng, Q., Wang, M., Zhu, T., Yu, E., Niu, J., Ge, X., Mao, D., et al., 2021. An effective brain imaging biomarker for AD and aMCI: ALFF in Slow-5 Frequency Band. Curr. Alzheimer Res.
Wang, H., Jin, X., Zhang, Y., Wang, J., 2016. Single-subject morphological brain networks: connectivity mapping, topological characterization and test-retest reliability. Brain Behav. 6, e00448.
Wang, Y., Xu, Q., Luo, J., Hu, M., Zuo, C., 2019. Effects of age and sex on subcortical volumes. Front. Aging Neurosci. 11, 259.
Wu, M.T., Tang, P.F., Tseng, W.I., Hsu, Y.C., Chen, Y.J., Goh, J.O.S., Chou, T.L., Chang, Y. K., et al., 2020. Integrity of the prefronto-striato-thalamo-prefrontal loop predicts tai chi chuan training effects on cognitive task-switching in middle-aged and older adults. Front. Aging Neurosci. 12, 602191.

Xing, Y., Yang, J., Zhou, A., Wang, F., Tang, Y., Jia, J., 2022. Altered brain activity mediates the relationship between white matter hyperintensity severity and cognition in older adults. Brain Imaging Behav. 16, 899–908.
Yu, M., Sporns, O., Saykin, A.J., 2021. The human connectome in Alzheimer disease - relationship to biomarkers and genetics. Nat. Rev. Neurol. 17, 545–563.
Zang, Y.F., He, Y., Zhu, C.Z., Cao, Q.J., Sui, M.Q., Liang, M., Tian, L.X., Jiang, T.Z., et al., 2007. Altered baseline brain activity in children with ADHD revealed by resting-state functional MRI. Brain Dev. 29, 83–91.
Zhang, N., Gordon, M.L., Ma, Y., Chi, B., Gomar, J.J., Peng, S., Kingsley, P.B., Eidelberg, D., et al., 2018. The Age-Related Perfusion Pattern Measured With Arterial Spin Labeling MRI in Healthy Subjects. Front. Aging Neurosci. 10, 214.